LI, F. H. & TANG, D. (1985). *Acta Cryst.* A41, 376–382.
SHANNON, R. D. & PREWITT, C. T. (1969). *Acta Cryst.* B25, 923–946.
SPENCE, J. (1980). *Experimental High Resolution Electron Microscopy*, pp. 85–88. Oxford Univ. Press.
WANG, P., PAN, Z. L., WENG, L. B., CHEN, D. C., ZHAO, A. X., CHEN, S. X., YE, Z. H., DONG, Z., XUE, J. Z., YANG, Z. Y. & LU, R. Y. (1984). *Systematic Mineralogy* (in Chinese), Vol. 2, pp. 380–394. Beijing: Geology Publishing House.
YADA, K. (1979). *Can. Mineral.* 17, 679–691.

Acta Cryst. (1989). B45, 136–141

A Transmission Electron Microscope Study of Modulated Sodium Lithium Metasilicates

BY R. L. WITHERS, J. G. THOMPSON AND B. G. HYDE

Research School of Chemistry, Australian National University, GPO Box 4, Canberra, ACT 2601, Australia

(*Received* 20 *July* 1988; *accepted* 24 *November* 1988)

Abstract

High-$Na_{2-x}Li_xSiO_3$, $0{\cdot}86 \le x \le 1{\cdot}02$, occurs as a modulated structure, the subcell of which is equivalent to the unit cells of Na_2SiO_3 and Li_2SiO_3 (orthorhombic, $Cmc2_1$), with the primary modulation wavevector directed along **b***. A satellite extinction condition observed at the [100] zone axis implies that the primary component of the incommensurate modulation involves an antiphase relationship between the modulations associated with sites related by a mirror plane perpendicular to the **a** axis. This antiphase relationship provides an explanation for the limited composition range of existence of this modulated phase. The modulation periodicity, while composition dependent, clearly can *not* be directly related to the Na : Li ratio. Less-rapidly cooled specimens show planar boundaries perpendicular to **b** and are interpreted as incipient high→low transition, resulting in breaking the above condition and streaking along **b***.

Introduction

An X-ray diffraction study of phase equilibria in the system $Na_2SiO_3 + Li_2SiO_3$ by West (1976, 1977) revealed a modulated structure for the phase he termed 'high-$(Na,Li)_2SiO_3$ solid solution'. It was produced by rapid quenching (in ~1 s) of approximately equimolar compositions, $Na_{2-x}Li_xSiO_3$ with $0{\cdot}86 \le x \le 1{\cdot}02$, from above ~1083 K; *i.e.* from just below the solidus to room temperature. Slower (air) cooling (in ~20 s) produced a phase of closely-related structure termed 'low-$(Na,Li)_2SiO_3$'. (Still slower cooling yielded phase mixtures of Na-rich and Li-rich solid solutions.)

High-$(Na,Li)_2SiO_3$ has a subcell identical to the unit cells of both Na_2SiO_3 and Li_2SiO_3: orthorhombic, space group $Cmc2_1$† (*cf.* Fig. 1). But its diffraction patterns contain additional, satellite reflections indicating a modulation along **b**. The Bravais lattice of low-$(Na,Li)_2SiO_3$ is a slight monoclinic distortion of this orthorhombic subcell: diffraction patterns contain no satellite reflections; but the product was invariably twinned on (100).

West (1977) reported that the magnitude of the primary modulation wavevector, **q**, characteristic of the high-$(Na,Li)_2SiO_3$ structure, varied linearly with composition (x in $Na_{2-x}Li_xSiO_3$), and was a rational number (corresponding to the existence of a superstructure) for simple Na/Li ratios; *e.g.* $\mathbf{q} = \mathbf{b}^*/6$ for Na/Li = 1 ($x = 1{\cdot}00$) and (slightly extrapolated) $\mathbf{b}^*/5$ for Na/Li = 5/4 ($x = 0{\cdot}89$). He commented that simple Na,Li ordering would not be expected to give such long-period superstructures. Nevertheless, the satellite reflections were attributed to long-range ordering of Na and Li (together with atomic displacements along **b***), an interpretation supported by the composition dependence of the magnitude of the modulation wavevector, $|\mathbf{q}|$, and occurrence of rational values of $|\mathbf{q}|$ for simple ratios Na/Li.

He also reported that the (single-crystal) diffraction patterns from some specimens showed considerable streaking in the **b*** direction, and suggested that it could be caused by very fine-scale incipient inversion pheno-

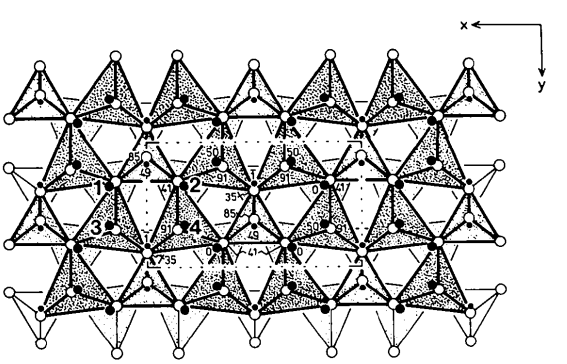

Fig. 1. Structure of Li_2SiO_3. The large tetrahedra are LiO_4 while the smaller tetrahedra are SiO_4. The unit cell is outlined and the four potential Na/Li sites per primitive unit cell are labelled 1 to 4.

† The standard setting; West (1976, 1977) used the nonstandard $Ccm2_1$.

0108-7681/89/020136-06$03.00

Table 1. *Refined unit- and subcell parameters (in Å) for high- and low-*$NaLiSiO_3$

Data in square brackets are from West (1976).

	a	*b*	*c*	β (°)	Volume (Å^3)
Low-$NaLiSiO_3$	9·771 (1)	5·7705 (9)	4·7720 (5)	91·24 (1)	269·00 (4)
	[9·86 (2)]	[5·73 (1)]	[4·77 (1)]	[91·5 (5)]	[269]
High-$NaLiSiO_3$, 'drop-quenched'	9·884 (5)	5·719 (2)	4·789 (1)		270·8 (2)
	[9·86 (1)]	[5·592 (5)]	[4·776 (5)]		268·0 (2)

mena associated with the high→low, orthorhombic→monoclinic transition.

The present paper reports the results of a transmission electron microscope study of the modulated, high-$(Na,Li)_2SiO_3$ phase, particularly the existence of an extinction condition on certain satellite reflections at the [100] zone axis, which provides insight into the nature of the modulation.

Experimental methods

Mixed silicate samples were prepared from analytical grade Li_2CO_3, Na_2CO_3 and SiO_2, largely following the procedures of West (1976, 1977). Our only departure from his method was to produce rapidly quenched specimens by dropping small (~50 mg) samples (sealed in Pt capsules, and annealed at 1093 K in a vertical tube furnace) into cold water, instead of mercury. These we term 'drop-quenched' specimens. Less-rapid quenching was achieved by cooling similar specimens in flowing, room-temperature air ('air-quenched'). Low-$(Na_{2-x}Li_x)SiO_3$ was produced from the 'high' form by cooling from 1093 K to room temperature over ~5 min.

All specimens were first characterized by X-ray powder diffraction, using a Guinier–Hägg camera and monochromated Cu $K\alpha_1$ radiation, with Si as an internal standard.

The composition range studied was that reported by West (1977) *viz.* $0{\cdot}86 \leq x \leq 1{\cdot}02$. The data presented here are mainly for the 'stoichiometric' sample with $x = 1{\cdot}00$, *i.e.* $NaLiSiO_3$, the results for its low and high forms being similar to those from other compositions.

Selected-area and convergent-beam electron diffraction patterns (SADP's and CBP's) were obtained from crushed specimens using Philips EM 430 and Jeol 100 CX electron microscopes. The material was readily damaged by the electron beam, an effect that was minimized by using a liquid-N_2 cold stage (in the EM 430), and by limiting the electron microscopy examination to medium-resolution images.

Results

Unit-cell dimensions for low-$NaLiSiO_3$ and (orthorhombic) subcell dimensions for high-$NaLiSiO_3$, calculated from X-ray powder diffraction data, are given in Table 1.

Typical [*h*01] and [100] zone-axis SADP's are shown in Figs. 2 and 3 respectively. Their general characteristics are in accord with West's (1977) report – stronger Bragg reflections from the $Cmc2_1$ subcell flanked by arrays of weaker satellite reflections. But the primary modulation wavevector **q** is $\mathbf{b}^*/5{\cdot}5$ rather than the value $\mathbf{b}^*/6{\cdot}0$ reported by West (1977) for this composition. To avoid compositional errors our samples were carefully prepared so as to be representative of much larger preparations, whose component weights determined the composition.

But this discrepancy, while puzzling (according to West it corresponds to 47·2 mol% Li_2SiO_3, *i.e.* $Na_{1{\cdot}05}Li_{0{\cdot}94}SiO_3$), is not of major concern to the main point of the present report. However, it is worth noting that we

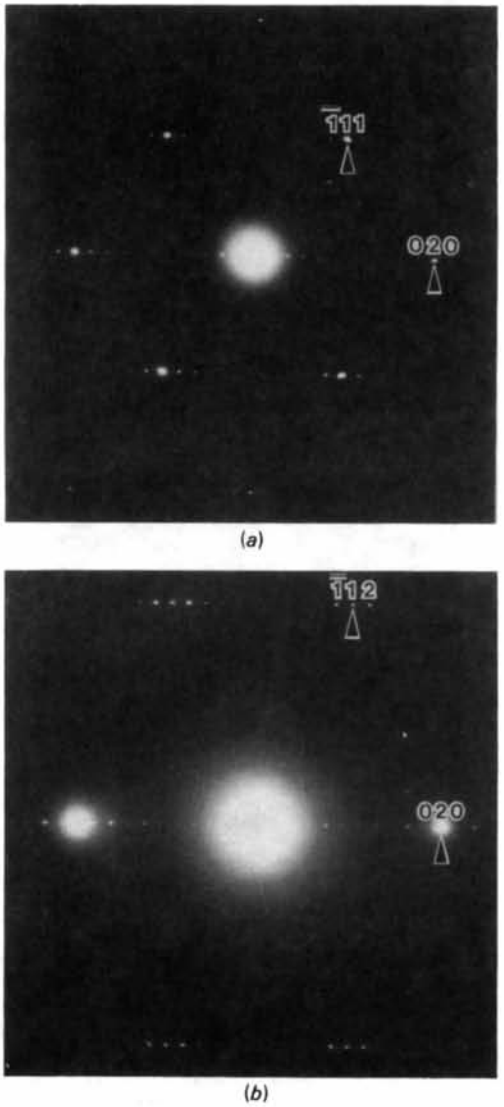

Fig. 2. Typical (*a*) [101] and (*b*) [201] zone-axis SADP's for high-$(Na,Li)SiO_3$.

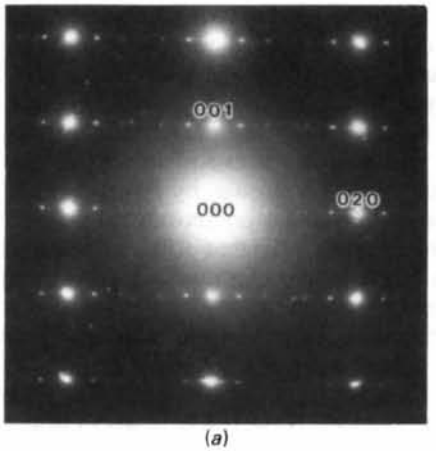

(*a*)

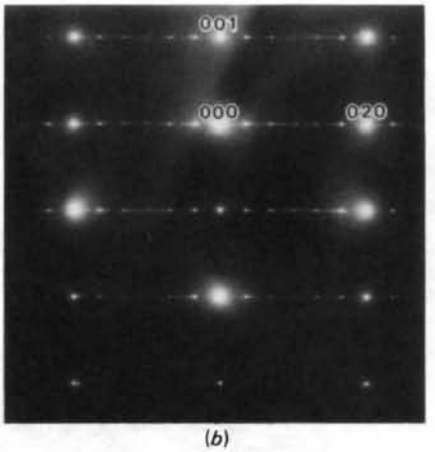

(*b*)

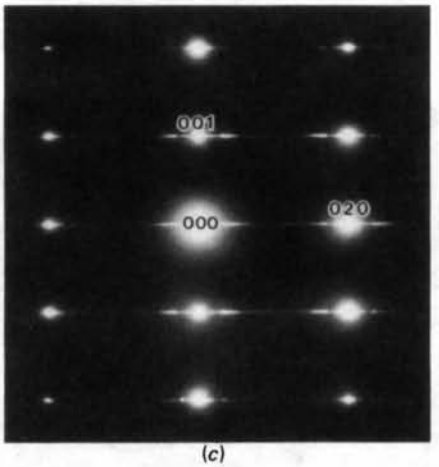

(*c*)

Fig. 3. [100] zone-axis SADP's showing progressively increasing disorder in the modulation. (*a*) A drop-quenched specimen exhibiting sharp matrix and satellite reflections. Note the absence of $\mathbf{G} \pm m\mathbf{q}$ (m odd) satellite reflections (*cf.* Fig. 2). (*b*) An air-quenched specimen. Notice the streaking along the $\mathbf{b}^*$ direction and the very weak presence of the $\mathbf{G} \pm m\mathbf{q}$ (m odd) satellite reflections. (*c*) An air-quenched specimen. The SADP is now heavily streaked and the sharp satellite reflections are absent.

did observe small variations in $|\mathbf{q}|$ from different crystals in the same preparation of our specimens.

Satellite intensity distribution

In Figs. 2(*a*) and 2(*b*) the $\mathbf{G} \pm m\mathbf{q}$ satellite reflections ($\mathbf{G}$ is an allowed subcell reciprocal lattice vector) are clearly present for $m = 1,2,3,\ldots$ Furthermore, the satellite intensities decrease monotonically as m increases. There is some variability in the [100] zone-axis SADP's as a function of quench rate, as shown in Fig. 3. For the drop-quenched specimen, the satellite reflections $\mathbf{G} \pm m\mathbf{q}$ are only visible when m is even, as shown in Fig. 3(*a*). That is, there is an extinction condition on the odd-m satellite reflections. For the air-quenched specimens, however, the odd-m satellite reflections are generally very weakly present, as shown in Fig. 3(*b*). Notice, however, that there is now quite a lot of streaking present also along the $\mathbf{b}^*$ direction. On rare occasions heavily streaked SADP's as shown in Fig. 3(*c*) occurred: in such cases, sharp satellite reflections were absent.

We have attempted to investigate the origin of this diffuse streaking along with the variability of the odd-m satellite extinction condition *via* real-space imaging of air-quenched specimens. Electron beam damage rules out high-resolution imaging. But by cooling the specimen and keeping the beam intensity low, it was possible to obtain reasonable resolution images at the [100] zone axis (see Fig. 4*b*). The ~16 Å fringes resulting from the strongest $2\mathbf{q}$ satellite reflections are visible along with planar boundaries perpendicular to $\mathbf{b}$ and spaced ~200–300 Å apart. It seems reasonable to suppose that these planar boundaries must be responsible both for the observed streaking along $\mathbf{b}^*$ as well as for the very weak presence of the odd-m satellite reflections at the [100] zone axis. The exact nature of the boundaries, however, is unclear. They may well be the twin boundaries reported for the monoclinic low form by West – although the structure is still metrically 'orthorhombic'. We believe that the absence of odd-m satellite reflections at the [100] zone axis in Fig. 3(*a*) is thus a genuine characteristic of well-ordered, high-$(Na,Li)_2SiO_3$.

Any mode amplitude associated with the odd-m modulation wavevectors (in particular with the primary modulation wavevector $\mathbf{q}$) must then transform according to that particular irreducible representation of the little cogroup (Bradley & Cracknell, 1972) of the modulation wavevector which gives rise to this observed satellite extinction condition (see, for example, Pérez-Mato, Madariaga & Tello, 1986; Withers, Hyde & Thompson, 1987).

Note that the existence of $\mathbf{G} \pm 2\mathbf{q}$ second-harmonic satellite reflections in the absence of the primary $\mathbf{G} \pm \mathbf{q}$ satellite reflections in the zero-order Laue zone (ZOLZ) at the [100] zone axis rules out double diffraction as the

origin of these observed satellite reflections and confirms the existence of a genuine second-harmonic modulation wave (West, 1977; Bird & Withers, 1986). West (1977) considered that this nonsinusoidality of the modulation waveform was more in keeping with a compositional, as opposed to a displacive, origin for the satellite reflections. It should be pointed out, however, that compositional modulation, in the form of Na/Li ordering, must also entail an accompanying displacive modulation (see, for example, Toman & Frueh, 1976).

We have attempted to investigate this question of the nature of the mode amplitudes associated with the various modulation wavevectors *via* large-angle higher-order Laue zone (HOLZ) scattering effects (see, for example, Steeds, Bird, Eaglesham, McKernan, Vincent & Withers, 1985). Fig. 5(*a*) shows an [010] zone-axis SADP and Fig. 5(*b*) the corresponding CBP. Note the matrix extinction condition, $F(h0l) = 0$ unless $h,l = 2n$, present in Fig. 5(*b*), consistent with a parent space group of $Cmc2_1$. [The weak presence of the space-group-forbidden, $l = 2n + 1$, reflections in the SADP of Fig. 5(*a*) is clearly an artefact due, presumably, to multiple scattering.] The only observed HOLZ ring is very close in and corresponds to a satellite HOLZ ring due to the primary modulation wavevector. The absence of any obvious azimuthal intensity variation in

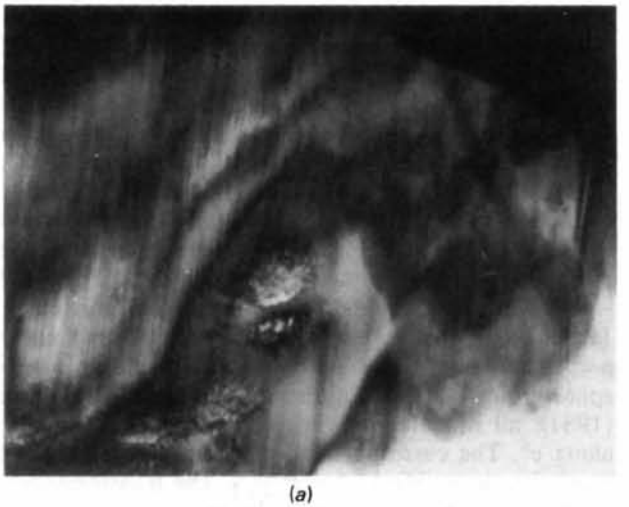

(*a*)

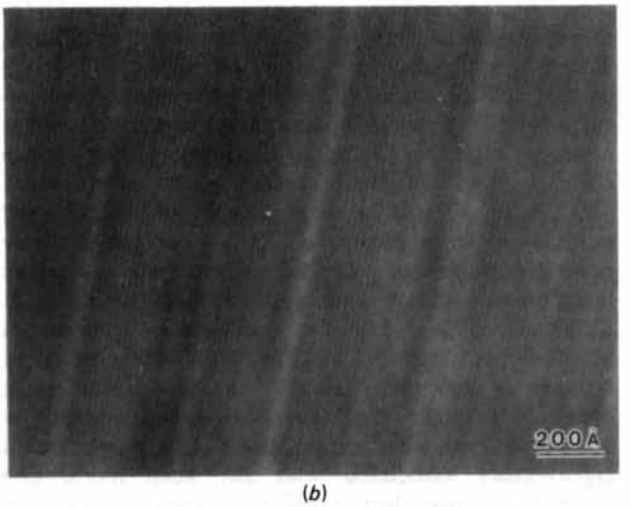

(*b*)

Fig. 4. (*a*) A low-magnification [100] zone-axis image of a grain which gave a heavily streaked SADP like that of Fig. 3(*c*). Note the planar boundaries perpendicular to **b** and spaced ~200–300 Å apart. (*b*) A higher-magnification image of a less-disordered region of this grain. Note the ~16 Å [$=(5.5/2)b$] fringes (corresponding to the $2\mathbf{q}$ modulation) in addition to the planar boundaries.

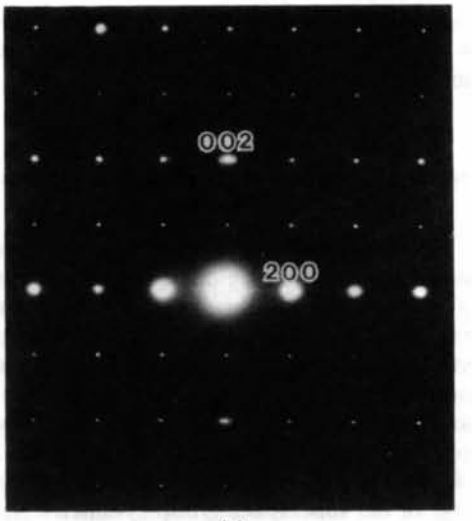

(*a*)

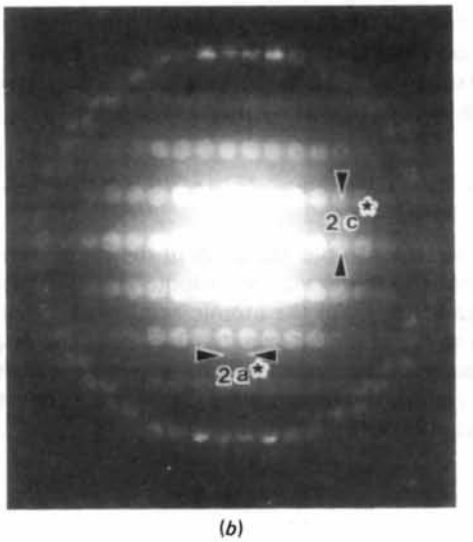

(*b*)

Fig. 5. An [010] zone-axis (*a*) SADP and (*b*) the corresponding convergent-beam pattern (CBP). Note the absence of any obvious azimuthal intensity variation in the satellite HOLZ ring of (*b*).

this satellite HOLZ ring, coupled with the general weakness of satellite HOLZ diffraction effects suggests that the modulations are primarily compositional in character (Pouget, 1980; Steeds *et al.*, 1985). This conclusion, however, needs to be tempered by the observation that the materials have a distinct tendency to beam damage. In particular, conventional electron beam intensities rapidly suppress the HOLZ rings observed at the [010] zone axis. Indeed excessive irradiation destroys the sublattice and turns the sample into a glasslike, amorphous state within a very few minutes. Nevertheless, whatever the relative contribution made by the compositional and displacive components to the mode amplitude associated with the primary modulation wavevector, it must still transform under the appropriate little group symmetry operation in such a way as to give rise to the observed satellite extinction condition.

Interpretation of the observed satellite extinction condition

Just as it is possible to derive general extinction conditions for ordinary three-dimensional space groups from a knowledge of the space-group symmetry elements, so it is also possible to derive general extinction conditions for incommensurate satellite reflections either from a knowledge of the transformation properties of the mode amplitudes associated with each modulation wavevector (Pérez-Mato *et al.*, 1986; Withers *et al.*, 1987) or, equivalently, from a knowledge of the superspace-group symmetry elements present (Pérez-Mato *et al.*, 1986; Pérez-Mato, Madariaga, Zuñiga & Garcia Arribas, 1987).

In general, the compositional component of the deviation from average symmetry due to the primary modulation (**q**) and possible higher-order harmonics (2**q**, 3**q**, ... *etc.*) can be written in the form:

$$\delta f_{l\kappa} = \bar{f}_\kappa \sum_{n=1}^{\infty} a_\kappa(n\mathbf{q}, \textstyle\sum_n)\cos[2\pi n\mathbf{q}.\mathbf{r}_l + \theta_\kappa(n\mathbf{q}, \textstyle\sum_n)], \quad (1)$$

where $l\kappa$ refers to the κth atom in the lth primitive unit cell and $\delta f_{l\kappa}$ represents a periodic deviation from its average value, $\bar{f}_\kappa$, of the atomic scattering factor of the κth atom site in the lth primitive unit cell. The displacive component of the deviation from average symmetry due to the various modulations (**q**, 2**q**, ... *etc.*) can similarly be written in the form:

$$\mathbf{U}_{l\kappa} = \sum_{n=1}^{\infty} \sum_{\alpha=x,y,z} \varepsilon_{\kappa\alpha}(n\mathbf{q}, \textstyle\sum_n) \times \cos[2\pi n\mathbf{q}.\mathbf{r}_l + \varphi_{\kappa\alpha}(n\mathbf{q}, \textstyle\sum_n)]. \quad (2)$$

In general, the compositional eigenvectors $\{A_\kappa(n\mathbf{q}, \sum_n) = a_\kappa(n\mathbf{q}, \sum_n)\exp[i\theta_\kappa(n\mathbf{q}, \sum_n)]\}$ are thus specified by $\kappa = 1 \rightarrow N$ complex numbers, one for each atom in the primitive parent unit cell, while the displacement eigenvectors $\{\mathbf{e}_\kappa(n\mathbf{q}, \sum_n) = \sum_\alpha \varepsilon_{\kappa\alpha}(n\mathbf{q}, \sum_n)\exp[i\varphi_{\kappa\alpha} \times (n\mathbf{q}, \sum_n)]\}$ are specified by x, y and z complex components for each of the N atoms per primitive unit cell. In the case of high-$(Na,Li)_2SiO_3$, however, the compositional modulation can only be associated with Na/Li ordering and thus the only possible nonzero compositional eigenvector components are associated with the four Na/Li sites per primitive parent unit cell (labelled 1 to 4 in Fig. 1). The average atomic scattering factor for each of these sites clearly depends upon stoichiometry *i.e.* upon x. If $x = 1$, for example, $\bar{f}_\kappa = 1/2(f_{Na} + f_{Li})$. Equation (1) then describes the compositional component of the deviation of the modulated structure from this average structure.

Modulation functions as given by equations (1) and (2) will, in general, give rise to satellite intensity at $\mathbf{G} \pm m\mathbf{q}$, where **G** is an *allowed* subcell reflection [*i.e.* $\mathbf{G} = (h,k,l) \equiv h\mathbf{a}^* + k\mathbf{b}^* + l\mathbf{c}^*$ and $(h+k) = 2n$] and m is any integer (see, for example, Yamamoto, 1982; Pérez-Mato *et al.*, 1987). The observed satellite extinction condition, $F(0,2k,l,m) \equiv F[(0,2k,l) + m\mathbf{q}] = 0$ unless $m = 2n$ (see Fig. 3*a*), is a consequence of the superspace-group symmetry operation $\{\sigma_x | \mathbf{0}, \tau = 1/2\}$ [see, for example, equation (5.9) of de Wolff, Janssen & Janner (1981)]. σ_x here represents a reflection in a plane perpendicular to the **a** axis. The corresponding superspace group is $P^{Cmc2_1}_{s\ \bar{1}\bar{1}}$. In the notation of de Wolff *et al.* (1981), all modulation wavevectors are chosen to be along **c***. The corresponding superspace group is thus listed therein as $36c.15.2 \equiv P^{A2_1ma}_{\bar{1}\ s\ \bar{1}}$. The transformation properties of the mode amplitudes associated with each modulation wavevector can similarly be obtained from the observed satellite extinction condition as follows. The isogonal point group, F, of any space group consists of the set of all rotational symmetry operations belonging to that space group. In the case of the average high-$(Na,Li)_2SiO_3$ structure (space group $Cmc2_1$), this isogonal point group $F = 2mm = \{E, C_2, \sigma_y, \sigma_x\}$. The little co-group, $\bar{G}^{\mathbf{q}}$, of the observed modulation wavevectors (**q**, 2**q**,...) consists of those point group symmetry operations belonging to F which leave the modulation wavevectors invariant (Bradley & Cracknell, 1972). For the modulation wavevectors observed in high-$(Na,Li)_2SiO_3$, this little co-group consists of only two elements – namely E and σ_x. In order to explain the observed satellite extinction condition, both the compositional and displacement eigenvectors associated with any such modulation wavevector must then transform according to one or other of the two irreducible representations of this little co-group, the multiplication table for which is given by:

	E	σ_x
$\sum_1$	1	$\bar{1}$
$\sum_2$	1	$\bar{1}$.

For $\{\sigma_x|\mathbf{0}, \tau = 1/2\}$ to be a superspace-group symmetry operation,

$$\chi^{\sum_2 n}(\sigma_x) = +1 \text{ for } n \text{ even}$$
$$= -1 \text{ for } n \text{ odd}. \quad (3)$$

Thus any compositional and displacement eigenvectors associated with the m-odd (*i.e.* $\mathbf{q}$, $3\mathbf{q}$, $5\mathbf{q}$,...) satellite reflections must transform with $\sum_2$ symmetry, while those associated with the m-even (*i.e.* $2\mathbf{q}$, $4\mathbf{q}$,...) satellite reflections must transform with $\sum_1$ symmetry.

The form of the deviation of the modulated structure from its average symmetry can then be obtained *via* application of (3). In the interests of brevity (and also because experimental evidence suggests that the ordering is primarily compositional in character) only the compositional components will be derived. We write a general such compositional eigenvector as

$$A = (A_1, A_2, A_3, A_4),$$

where the four complex numbers A_1 to A_4 are the compositional eigenvector components associated with the four possible Na/Li sites per primitive unit cell (see Fig. 1). Under $\{\sigma_x|\mathbf{0}\}$,

$$A \rightarrow (A_2, A_1, A_4, A_3) = A\chi^{\sum_2 n}(\sigma_x).$$

For the odd-$\mathbf{q}$ modulations ($\mathbf{q}$, $3\mathbf{q}$, ...), $\chi^{\sum_2 n}(\sigma_x) = -1$ and therefore

$$A = (A_1, -A_1, A_3, -A_3),$$

i.e. any increase in the atomic scattering factor on sites 1 or 3 is matched by an equal and opposite decrease in the atomic scattering factor on the σ_x-symmetry-related sites, *i.e.* sites 2 and 4. To put it another way, if site 1 is filled by an Na atom then site 2 will tend to be filled by an Li atom and *vice-versa*. This perhaps explains the limited composition range of existence (around Na:Li$\simeq$1:1) of this modulated phase. For the even-$\mathbf{q}$ modulations, $\chi^{\sum_2 n}(\sigma_x) = +1$ and thus $A = (A_1, A_1, A_3, A_3)$; *i.e.* any increases in the f's of sites 1 and 3 are matched by an equal increase in the f's of sites 2 and 4. In general,

$$\delta f_{l,\kappa=1} = \bar{f}_\kappa \{1 + a_1(\mathbf{q}, \sum_2)\cos[\mathbf{q}.\mathbf{r}_l + \theta(\mathbf{q}, \sum_2)]$$
$$+ a_1(2\mathbf{q}, \sum_1)\cos[2\mathbf{q}.\mathbf{r}_l + \theta_1(2\mathbf{q}, \sum_1)] + \ldots\}$$

$$\delta f_{l,\kappa=2} = \bar{f}_\kappa \{1 - a_1(\mathbf{q}, \sum_2)\cos[\mathbf{q}.\mathbf{r}_l + \theta_1(\mathbf{q}, \sum_2)]$$
$$+ a_1(2\mathbf{q}, \sum_1)\cos[2\mathbf{q}.\mathbf{r}_l + \theta_1(2\mathbf{q}, \sum_1) + \ldots\} \quad (4)$$

It will be the task of a full X-ray structure determination to evaluate the amplitudes and phases of these various harmonics, as well as for their displacive counterparts.

Conclusions

(i) The primary component of the incommensurate modulation involves an antiphase relationship between the modulations of σ_x-symmetry-related sites, *i.e.* if site 1 is filled by an Na atom then site 2 will tend to be filled by an Li atom and *vice-versa*.

(ii) This antiphase relationship of the σ_x-symmetry-related sites provides an explanation for the limited composition range of existence (around Na:Li $\simeq$ 1:1) of this modulated phase.

(iii) The modulation periodicity ($\sim 6\mathbf{b}$), while composition dependent, clearly can *not* be directly related to the Na–Li ratio.

References

BIRD, D. M. & WITHERS, R. L. (1986). *J. Phys. C*, **19**, 3497–3505.

BRADLEY, C. J. & CRACKNELL, A. P. (1972). *The Mathematical Theory of Symmetry in Solids*. Oxford: Clarendon Press.

PÉREZ-MATO, J. M., MADARIAGA, G. & TELLO, M. J. (1986). *J. Phys. C*, **19**, 2613–2622.

PÉREZ-MATO, J. M., MADARIAGA, G., ZUÑIGA, F. J. & GARCIA ARRIBAS, A. (1987). *Acta Cryst.* A**43**, 216–226.

POUGET, J. P. (1980). *Solid State Phase Transformations in Metals and Alloys*, p. 523. Orsay: Editions de Physique.

STEEDS, J. W., BIRD, D. M., EAGLESHAM, D. J., MCKERNAN, S., VINCENT, R. & WITHERS, R. L. (1985). *Ultramicroscopy*, **18**, 97–110.

TOMAN, K. & FRUEH, A. J. (1976). *Acta Cryst.* B**32**, 521–525.

WEST, A. R. (1976). *J. Am. Ceram. Soc.* **59**, 118–121.

WEST, A. R. (1977). *Acta Cryst.* A**33**, 408–411.

WITHERS, R. L., HYDE, B. G. & THOMPSON, J. G. (1987). *J. Phys. C*, **20**, 1653–1669.

WOLFF, P. M. DE, JANSSEN, T. & JANNER, A. (1981). *Acta Cryst.* A**37**, 625–636.

YAMAMOTO, A. (1982). *Acta Cryst.* A**38**, 87–92.